

Development of a CryoMAS™ HR-MAS-MAG NMR Probe for High-field WB Magnets

Sid Shevgoor, JB Spitzmesser, Jatin Kulkarni, John P. Staab, George Entzminger, and F. David Doty

Doty Scientific, Columbia, SC

ABSTRACT

HR NMR probes for liquids have recently become available with cryogenically cooled sample coils that promise major advances in the field of NMR owing to their factor of four improvement in SNR. Even greater improvements in SNR may be possible in High-Resolution (HR) Magic Angle Spinning (MAS), which extends NMR techniques to inhomogeneous systems, such as human and animal tissues, and solids.

The goal of this major, long-term development effort is to ultimately achieve an order of magnitude gain in S/N in HR-MAS variable temperature (VT) NMR probes for NMR spectroscopy of inhomogeneous systems and many solids. Cryo-coil probes achieve their improvement in SNR from the combined effects of reduced noise temperature and improved Q, in spite of their reduced magnetic filling factor. In addition to improved S/N for samples near RT, the CryoMAS probe may ultimately allow the sample VT range to extend from 30 K to 400 K while the RF coils and capacitors are kept at ~30 K.

The engineering challenges of developing a CryoMAS probe (HR-MAS with full-range VT capability and Magic Angle Gradient) are substantial but not insurmountable. Preliminary circuit analyses show that a combination of (1) a novel approach to quadrature MAS (^1H - ^{13}C - ^1H - ^{15}N) with all of the critical circuit elements maintained at ~30 K, (2) integrating a ceramic dewar into a novel sample spinner design, and (3) cryogenic preamps offers the potential for an order of magnitude increase in SNR in an MAS probe for many applications. Hence, signal averaging time may be reduced by up to two orders of magnitude. The extended cryogenic sample range of the probe will permit further gains in SNR for many solids applications.

We report our progress toward demonstrating feasibility of a dewared 3 mm MAS spinner design with a high-efficiency quadrature cryogenic circuit for use at fields up to 800 MHz.

INTRODUCTION AND BACKGROUND

Our primary objective is to decrease NMR acquisition time in an HR-MAS probe by more than an order of magnitude as a result of increasing the SNR by a factor of at least four. This will be accomplished by cooling the RF sample coil and other key RF components to about 30° K.

The basis for the expected improvement in sensitivity comes from the following equation for SNR expressed in terms of NMR parameters [1]:

$$S/N = \left[\frac{\hbar^2 \sqrt{2\pi} I_0}{12k_B^2} \right] \left[\frac{n_s \gamma^2 I_x (I_x + 1) \sqrt{f_2}}{T_s \sqrt{T_R + T_p}} \right] \left[\eta_e \eta_f Q_L V_s \right]^{1/2} \omega^2 \quad (1)$$

where \hbar is Planck's constant, μ_0 is the permeability of free space, k_B is Boltzmann's constant, n_s is the number of spins at resonance per unit volume, γ is the magnetogyric ratio, I_x is the spin quantum number, T_s is the spin-spin relaxation time, T_p is the sample temperature, T_R is the temperature of the circuit resistance (coil and capacitors), T_p is the effective pre-amp noise temperature, η_e is the RF efficiency, η_f is the magnetic filling factor, Q_L is the loaded circuit quality factor, V_s is the sample volume, and ω is the Larmor precession frequency, γB_0 .

Assuming n_s , γ , I_x , B_0 , T_s , T_p , and V_s remain fixed (as for a given experiment), the gain in SNR is expected to come primarily from a reduction in $(T_R + T_p)$ by initially a factor of ~7 and an increase in Q_L by a factor of ~7 (ultimately, both the coil and capacitor Qs may increase by more than a factor of 8 [2]). The reduction in η_e of about 30% that stems from the addition of a dewar between the RF coils and the sample (needed to keep the coils cold while the sample is warm) will be offset by improved RF circuit efficiency — i.e. reduced relative losses in the coils, leads, and capacitors needed to achieve the multiple resonances.

Careful attention to many details will be required to actually realize the expected improvement in SNR. Because the electron mean free path in cold copper (below ~50 K) is large compared to the classical fit skin depth, cooling below ~40 K does not result in much additional increase in the Q of the coil. Also, in this regime, aluminum achieves better Q than copper, especially in high fields, where copper's magneto-resistance is quite significant. Specially fabricated coaxial sapphire capacitors will be required to achieve an order of magnitude increase in capacitor Qs compared to standard RF capacitors.

Besides providing a factor of 4 to 9 improvement in SNR, other complex features are being included. The probe is being designed with up to 4 fixed channels (^1H - ^{13}C - ^1H - ^{15}N), allowances will be made for a magic-angle gradient (MAG) coil, and the probe will have VT capabilities (our ultimate VT goal is to control the sample temperature over the range of 30 to 400°K). All of this must be accomplished in a probe with a 72.6 mm outside diameter and a cold region heat leak sufficiently small to keep the operating and equipment costs reasonable.

Initial 35 K tests are still about 5 months away. The work presented here includes: (1) a preliminary design of the cold region surrounding the spinner (the probe head), (2) an initial spinner design, (3) the results of thermal analyses conducted on the spinner assembly and probe head, and (4) a preliminary RF circuit.

PRELIMINARY DESIGN OF PROBE HEAD

The mechanical design work to date has focused mostly on designing the top of the probe, including the spinner assembly and the chamber that houses all of the cooled RF components (except for the pre-amps). A cross section drawing through the spinner assembly with the Magic Angle Gradient (MAG) coil can be seen in Figure 1, and 3D renderings of the probe head are shown in Figures 2 and 3 with the bell-dewar shield and its attached insulation removed. All of the critical RF components, including the RF sample coils, are contained in a region that can be sealed to high-vacuum standards and pressurized with helium gas to inhibit any leaks from the drive/bearing gas flows.

Two-stage cooling is used. Cold nitrogen gas, at about 90 K, is used to minimize the amount of 30 K cooling power required. Conduction from a commercial cold finger containing a helium gas heat exchanger, very similar to that used in HR liquids cryo-probes, is then used to cool the components and sample coils to 30-35 K. The design reduces the heat leaks and allows for effective isolation of the effect of pressure pulsations in the cryocooler. Some of the components responsible for insulating the cold region from the surrounding warm regions can be seen in Figure 3.

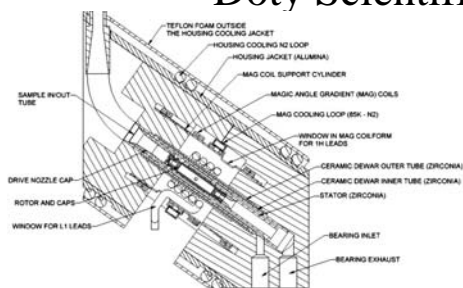
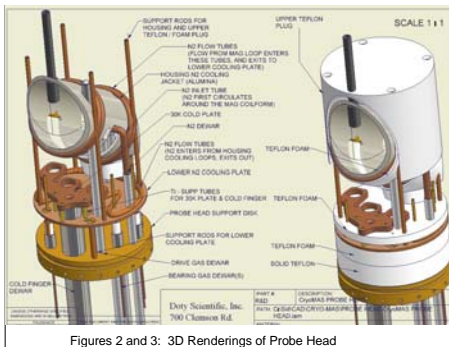


Figure 1. Probehead cross section through MAS spinner.

PRELIMINARY SPINNER DESIGN

One key element of the probe design is the development a spinner assembly for a 3 mm (outside diameter) rotor that can spin at 26 kHz, allow for automatic change of rotors, and maintain a sample temperature ranging from 30-400° K while the RF coils wrapped around its outside are kept at 35° K. A preliminary design of the spinner is shown in the cross section drawing of Figure 4. Due to the constraints imposed by the provisions for automatic sample eject and the dewar between the stator and the cold RF coil, the rotor is driven from one end only. We are currently optimizing the design of a 4 mm single-end-drive spinner assembly to achieve stable spinning at the highest possible speed. This design will be scaled down to a 3 mm design to accommodate smaller sample volumes. The 3 mm design is expected to spin up to 26 kHz.



Figures 2 and 3: 3D Renderings of Probe Head

The spinner employs a radial inflow micro-turbine similar to that shown in Figure 5, which is driven by a ring of nozzle holes in the nozzle cap. The bearing gas may ultimately range in temperature from 30-400 K to accommodate variable temperature experiments. By controlling the temperature of both the bearing and the drive, the thermal gradients in the sample can be minimized. Ceramic as well as plastic turbines are under development. The turbines are being optimized using advanced CFD (computational fluid dynamics) software. Figure 6 shows relative velocity vectors from CFD for supply pressure of 515 kPa and spin rate of 25 kHz. The blade length in the axial (span) direction is 1.0 mm. These radial-inflow blades are self shrouded and achieve up to ~35% isentropic efficiency. The frictional load for the 3 mm cryo-coil rotor at RT with radial and axial nitrogen-gas bearings is expected to be ~8 W at 18 kHz. With one micro-turbine at ~0.4 g/s N_2 , turbine efficiency needs to be ~20%. The novel radial inflow turbine shown in Figure 5 allows us to spin over 21 kHz in a 4 mm rotor with a single-end drive. Improvements in this design may increase the speeds to 24 kHz. Scaling this design to 3 mm will help us achieve 26 kHz spinning speeds, and other improvements are being made to reduce frictional sample heating at these speeds.

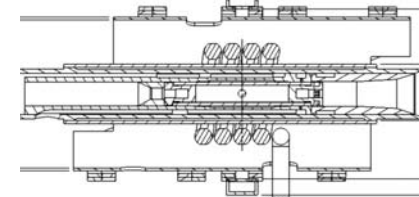


Figure 4: Cryo-Spinner Cross Section.

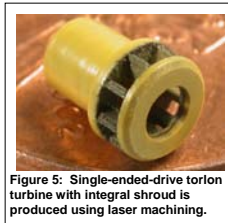


Figure 5: Single-ended-drive rotor turbine with integral shroud blades produced using laser machining.

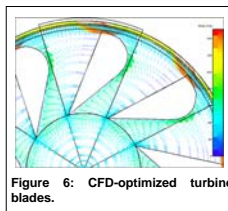


Figure 6: CFD-optimized turbine blades.

THERMAL ANALYSIS

To achieve the desired SNR, the RF coils (which are wrapped around the spinner) must be kept at about 35° K or lower. Meanwhile, the bearing and drive gas powering the spinner will be controlled over the range of 30-400° K for VT experiments. With these large thermal gradients in the spinner region, great care must be taken in the design to minimize the heat leaks and avoid prohibitive operating and siting costs.

One of the keys to limiting the heat transfer is the ceramic dewar located between the warm gas inside the stator and the cold RF coil. As Figure 4 shows, the ceramic dewar consists of two concentric ceramic tubes connected to a vacuum line that will continually pump the dewar while the probe is in use. The heat conduction along the dewar tube walls and through the dewar seals must be minimized, and high strength and good wear resistance are required elsewhere in the stator. To minimize thermal strain, all of the spinner-assembly components must be made from the same ceramic, and partially stabilized zirconia appears to have the best balance of properties here.

The dewared external shield will minimize the heat leaks into the probe head. Special low-magnetism, low-thermal-conductivity alloys will be used to minimize the heat conduction along the inner wall of this dewar without introducing problematic, temperature-dependent B_0 shifts. The critical RF elements within the probe head will be covered with a thin layer of foamed Teflon to reduce convective surface losses.

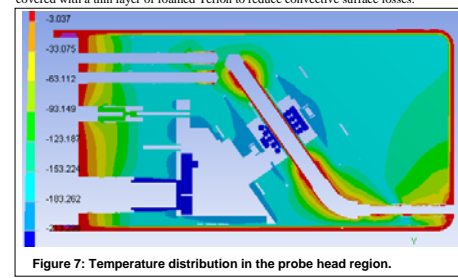


Figure 7: Temperature distribution in the probe head region.

The temperatures in the cold zone shown in Figure 7 were obtained from 3D FEA simulations using ANSYS DesignSpace software. The mean steady state temperature of the helium gas inside the probe head is ~70 K, though it approaches 35 K near the surface of the rf circuit components, which are shown more clearly in Figure 8, below. The dewar insulation around the cold finger is of extreme importance. The total heat leak to the cold finger must be kept under 7 W to be able to reach 30° K on the cold finger without major, expensive changes from existing cryo-probe equipment.

The top end of the probe head is insulated by the closed end of the shield bell-dewar, which has a port for the sample entry/eject tube. The heat loss through this ported bell-dewar is very small compared to other alternatives. The closed bell-dewar also simplifies the sealing at the top of the probe, with o-ring seals needed only around the base of the bell dewar.

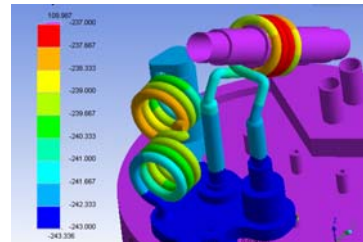


Figure 8: Calculated temperatures on several circuit components, including the sample coil, which is conduction cooled via sapphire capacitors.

HIGH PERFORMANCE CRYO-COIL RF CIRCUITS

As with most Doty solids probes, this probe will utilize the patented Doty Cross-Coil (XC) technology. The basic concept is to use a highly optimized saddle coil for the high frequency (^1H) channel and a separate, double-tuned solenoidal coil for the low frequency (LF) and mid-frequency (MF) channels (^{13}C and ^{15}N). A second (and less efficient) saddle coil that is orthogonal to the ^1H coil may also be added to accommodate the ^1H (lock) channel with relatively little performance degradation of the other coils. Placing the high and low frequency channels on separate orthogonal coils makes it much easier to optimize the RF solenoid circuit for one or two low frequency nuclei. The XC can then be optimized such that B_0 homogeneity, efficiency, and power handling are all improved relative to the single-coil approach [4, 5].

The separate circuits for the high and low frequency channels are shown in Figures 9 and 10. Note that the separate ^1H lock channel is not shown in these schematics. In both of these figures, the components above the dashed lines will be located in the cold zone while the variable capacitors shown below the dashed lines will be kept at room temperature due to their lubricated components.

The Q of the fixed capacitors in these circuits is critical to achieving the needed improvement in SNR. For some small capacitors, adequate capacitor Q (3000-9000) may be obtained by simply paralleling small chip capacitors, as the lower-value capacitors have higher Q. However, at least two (usually three) specially fabricated coaxial sapphire capacitors (C7, C11, C15) will be needed to achieve the desired LFMF performance.

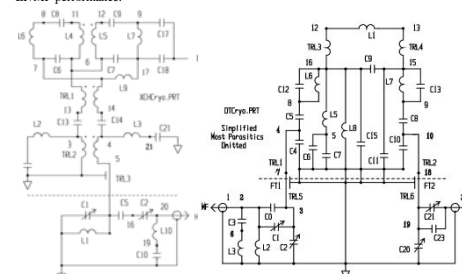


Figure 9: High Frequency Cross-Coil Circuit. Figure 10: ^{13}C and ^{15}N Double Tuned Solenoid Circuit.

Other possibilities for small-value capacitors include single layer devices made (in house) on copper-clad Teflon, quartz, or alumina substrates. Care must also be taken when selecting the type of solder used for attaching the capacitors, as the conductivity of standard solders is quite low and does not improve much at low temperatures.

In the high frequency circuit, C6-C9 are mounted very close to the Cross-Coil (L4-L7). C1 and C2 are variable capacitors used for tune and match. TR1-TR2 form leads, while TR3 represents a feed-through from the warm region to the cold. The impedance transformations in the coupling capacitors (C13, C14) keep the total signal loss in the warm components to just a few percent of that in the cold zone (which is quite small). This limits the tuning range to ~1%, which is sufficient for this ultra-low-E-field balanced ^1H coil.

In the LFMF circuit, L1 is the sample solenoid coil; TR3 and TR4 are leads; C12, C13, L6, and L7 are HF traps (if needed); C4, C5, C7, C8, C9, C10, L5, and L8 establish the two isolated resonances (^{15}N and ^{13}C) and appropriate impedance transformations; and TR1 and TR2 are the thermal-barrier feed-throughs. Again, the transformations insure that the total signal loss from the warm components (the LF and MF variables, C1, C2, C20, C21, L2, etc.) is but a few percent of that in the cold zone. The tuning ranges of the LF and MF circuits then are also each just ~1%. The sapphire coaxial capacitor capacitors C11 and C15 also serve as thermal links to the cold plate for conduction cooling of the various components.

CONCLUSIONS

We have begun the development of a CryoMAS™ HR-MAS-MAG probe that has the potential to increase SNR ultimately by nearly an order of magnitude and thus decrease acquisition time by nearly two orders of magnitude. Initial designs of the probe head, spinner assembly, and circuit have been completed. Thermal analysis, circuit simulation, and construction of a spinner prototype are currently well underway, and three related patent applications have been filed. Initial tests are expected within five months.

REFERENCES

1. F. D. Doty, "Probe Design and Construction," *The Encycl. of NMR Vol. 6*, Wiley, 3753-3762, 1996.
2. W. A. Anderson, "High Q Normal Metal NMR Probe Circuits," presented at the 42nd ENC, Orlando FL, 2001.
3. F. D. Doty, L. G. Hacker, and J. B. Spitzmesser, US Pat # 5,508,615, 1996.
4. F. D. Doty, G. Entzminger, and A. Yang, "Magnetism in HR NMR Probe Design, Part II: HR-MAS," *Concepts in Magn. Reson.*, (4), 239-260, 1998.
5. F. David Doty, George Entzminger Jr., and Cory D. Hauck, "Error-Tolerant RF Litz Coils for NMR/MRI," *J. Magn. Reson.*, 140:17-31, 1999.

Acknowledgements: This work supported by NIH R43 EB00152-02.